

03/24/97

C.O. #003 ACKNOWLEDGES REQUESTED 'REDUCTION' IN FUNDING FROM \$57,670 TO \$35,000.

4  
(7)

Closeout Notice Date 30-APR-1997

Project Number E-25-L90

Doch Id 37479

Center Number 10/24-6-R0221-0A0

Project Director GLEZER, ARI

Project Unit MECH ENGR

Sponsor MCDONNELL DOUGLAS CORP/ST LOUIS, MO

Division Id 4338

Contract Number Z51268

Contract Entity GTRC

Prime Contract Number F33615-94-C-3000

Title SYNTHETIC JETS FOR THRUST VECTOR CONTROL

Effective Completion Date 15-MAR-1997 (Performance) 15-MAR-1997 (Reports)

Closeout Action:	Y/N	Date Submitted
Final Invoice or Copy of Final Invoice	Y	03-MAR-1997
Final Report of Inventions and/or Subcontracts	Y	
Government Property Inventory and Related Certificate	Y	
Classified Material Certificate	N	
Release and Assignment	Y	01-APR-1997
Other	N	

Comments

Distribution Required:

Project Director/Principal Investigator	Y
Research Administrative Network	Y
Accounting	Y
Research Security Department	N
Reports Coordinator	Y
Research Property Team	Y
Supply Services Department	Y
Georgia Tech Research Corporation	Y
Project File	Y

NOTE: Final Patent Questionnaire sent to PDPI

# SYNTHETIC JETS FOR THRUST VECTOR CONTROL

Final Report MDA Contract Z51268

Ari Glezer

Woodruff School of Mechanical Engineering  
Georgia Institute of Technology

## I. Overview

A novel approach to the manipulation and control of shear flows using fluidic actuators based on synthetic jets has been developed at Georgia Tech. Such jets have the unique property of being zero-mass-flux in nature; i.e., they are synthesized from the working fluid in the flow system in which they are embedded. Although there is no net mass injection into the overall system, the jets allow momentum transfer into the embedding flow. The interaction of synthetic jets and an embedding flow near the flow boundary can lead to the formation of closed recirculation regions and thus an apparent modification of the flow boundary. These features enable synthetic jets to effect significant global modifications in embedding flows on scales that are one to two orders of magnitude larger than the characteristic length scale of the jets themselves. Earlier investigations supported by AFOSR demonstrated the utility of millimeter-scale synthetic jets actuators for the manipulation of a larger, centimeter-scale conventional primary jet. It was shown that the primary jet can be vectored without the use of mechanical actuators or control surfaces. The goal of the present work was to determine the scaling of the vectoring angle with other flow parameters.

## II. Scaling of Jet Vectoring

Because synthetic jets are zero-mass-flux in nature and are comprised entirely of entrained fluid, their interaction with an embedding flow near the flow boundary can result in the formation of low-pressure, recirculating flow regions and thus in an apparent modification of the flow boundary and turning of the embedding flow.

A conventional rectangular jet having emanating out of a 7.62 x 1.27 cm and 71cm long aluminum conduit is instrumented with two synthetic jet actuators each having an orifice plate measuring 0.5 x 75 mm and mounted along the long side of the primary jet conduit as shown schematically in Figure 1a. The downstream end of the facility including the actuators and the coordinate system are shown schematically in Figure 1b. The rectangular conduit is centrally mounted on the downstream endplate of a cylindrical

plenum tube. No contraction is used, and an azimuthally uniform bleeding gap along the perimeter of the plenum tube (Figure 1b) is adjusted until the velocity distribution across the plenum tube just upstream of the inlet of the conduit is approximately uniform. This minimizes secondary flow at the inlet and along the corners of the square conduit and, as a result, the turbulence level at the jet exit. The jet is driven by an axial blower powered by a DC motor and jet velocities up to 20 m/sec can be realized. In the experiments described below the centerline velocity of the primary jet is 7 m/sec corresponding to a  $Re_H \approx 6,000$ . The streamwise and cross-stream velocity components are measured using two-component hot wire anemometry. The hot wire probe is mounted on a computer-controlled three-axis traversing mechanism and most of the measurements are taken in the x-y plane  $z = 0$  within the streamwise domain  $0 < x/H < 11.8$ .

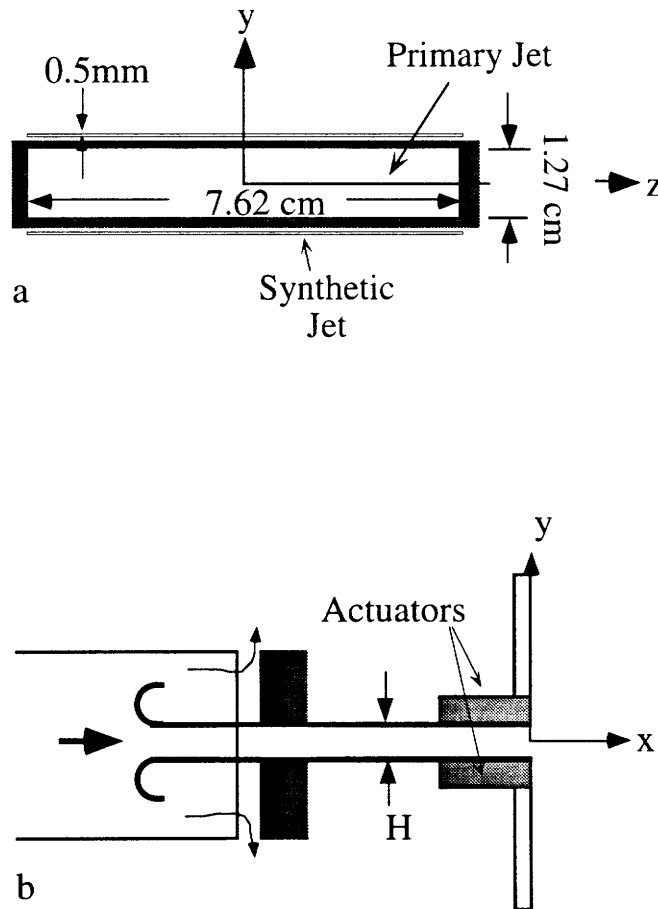


Figure 1

Using the actuator arrangement described above, the primary jet can be vectored either *toward* or *away* from each of the synthetic jet actuators. These two vectoring modes are very different in nature and are denoted “pull” and “push” mode respectively. In the “pull” mode the synthetic jet is nominally collinear with the primary jet, while in the “push” mode the synthetic jet impinges normal to and along the span of the primary jet. The vectoring of the primary jet is shown in a sequence of Schlieren images in Figures 2a-d. The Schlieren view is in the x-y plane (along the span of the primary jet) and consists of a 15.2 cm diameter circle, centered around  $x/H = 4$ . The primary jet is visualized by slight heating of the jet fluid above the ambient. A sketch of the jet conduit and the top and bottom actuators is shown schematically on the left hand side of each image. The unforced primary jet is shown for reference in Figure 2a, and the (symmetric) roll up of spanwise vortices in the upper and lower jet shear layers is clearly visible. When the top actuator is activated in the pull mode, the primary jet is vectored towards the actuator (Figure 2b). There is no question that the vectoring is accompanied by a substantial increase in small-scale motions within the primary jet and that the forcing impedes the evolution of the spanwise vortices in Figure 2a. The bottom actuator is operated in the push mode and, as a result, the primary jet is vectored away from the actuator at an angle that is roughly comparable to that of the pull mode (Figure 2c). If both actuators are operated in concert, the primary jet can be vectored at substantially larger angles (Figure 2d). In the present paper, we restrict our attention to pull mode vectoring only.

The mean streamlines of the vectored jet in the cross stream plane  $z = 0$  are computed from measurements of the streamwise and cross stream velocity components on a rectangular grid within the domain  $-2.3 < x/H < 1.6$  (within the conduit, the cross stream extent of the measurement domain is  $-0.28 < y/H < 0.28$ ). The streamlines shown in Figure 3 start at  $x/H = -2.3$  where the flow within the conduit is nominally parallel and the value of the stream function increases by equal increments between adjacent streamlines. The primary jet conduit is also shown schematically for reference. These streamlines clearly indicate that at least in the center plane  $z = 0$ , the jet begins to vector within the conduit for  $x/H > -1$  indicating the presence of unequal static pressure distributions on the top and bottom surfaces of the conduit. It is also noteworthy that the turning of the flow is almost complete within less than  $1/2$  the jet width ( $x/H < 0.4$ ) downstream of the exit plane.

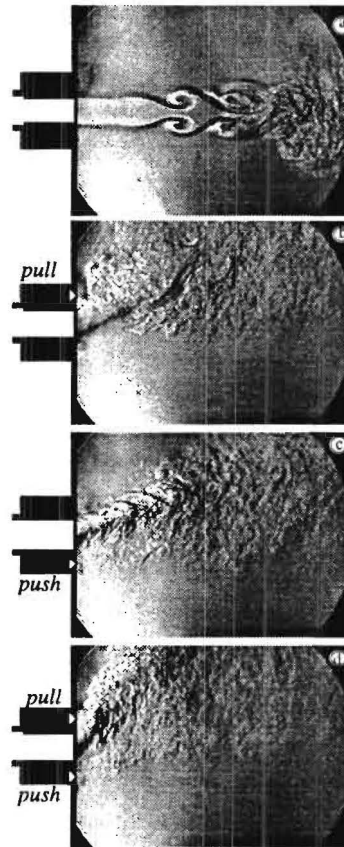


Figure 2

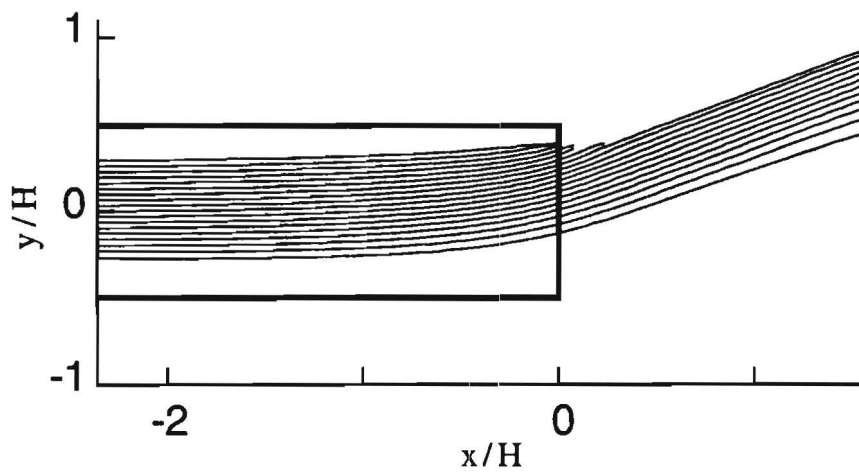


Figure 3

In the measurements reported above the ratio of the cross-stream momentum flux of each (primary and synthetic) jet is kept invariant. In what follows, the effect of this momentum ratio on the degree of vectoring of the primary jet is investigated. To this end, the vectoring angle  $\alpha$  along a *single* streamline that originates at the centerline of the jet conduit  $y = z = 0$  (well upstream of where the vectoring effects begins) is directly measured using an X-wire sensor. By continuously computing the time-averaged streamwise and cross-stream velocity components, the sensor is traversed (using small step size  $0.04H$ ) downstream in the cross stream plane tangent to the local flow vector and ostensibly along the same streamline. The present measurements were taken in the streamwise domain  $-2.4 < x/H < 0.78$ . Figure 4 shows the center streamline for  $4.4 < P < 23.3$  (where the centerline velocity of the primary jet is fixed at 7 m/s while the momentum flux of the synthetic jet is varied). As might be expected, small values of  $P$  result in large vectoring angles.

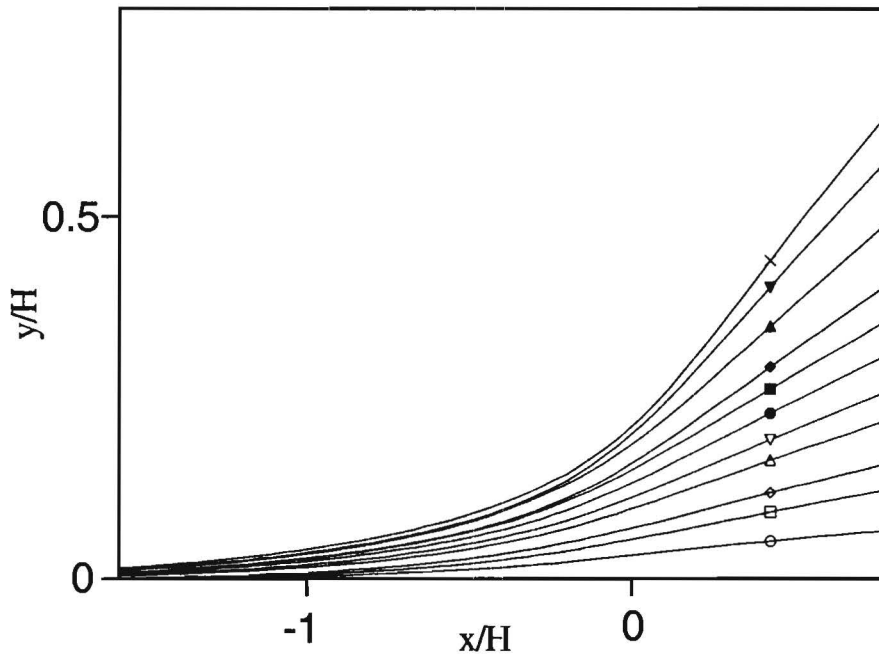


Figure 4

The momentum ratio alone does not uniquely determine the vectoring angle (for a given flow geometry). Figures 5a shows two center streamlines for which  $P = 4.8$  but where the velocity of the primary jet is different (5 and 7 m/sec corresponding to the solid and dashed lines). Figure 5b shows the curvature of the streamlines and amplifies subtle details such as the onset of vectoring and the small relaxation near  $x/h=0.5$  in many of the

cases. The streamline curvature also provides a convenient length scale that is associated with the vectoring that can be related a characteristic time scale. There is no question that the streamlines in Figures 5a and b are not the same and that for a given momentum ratio, the vectoring angle increases with the momentum of the primary jet.

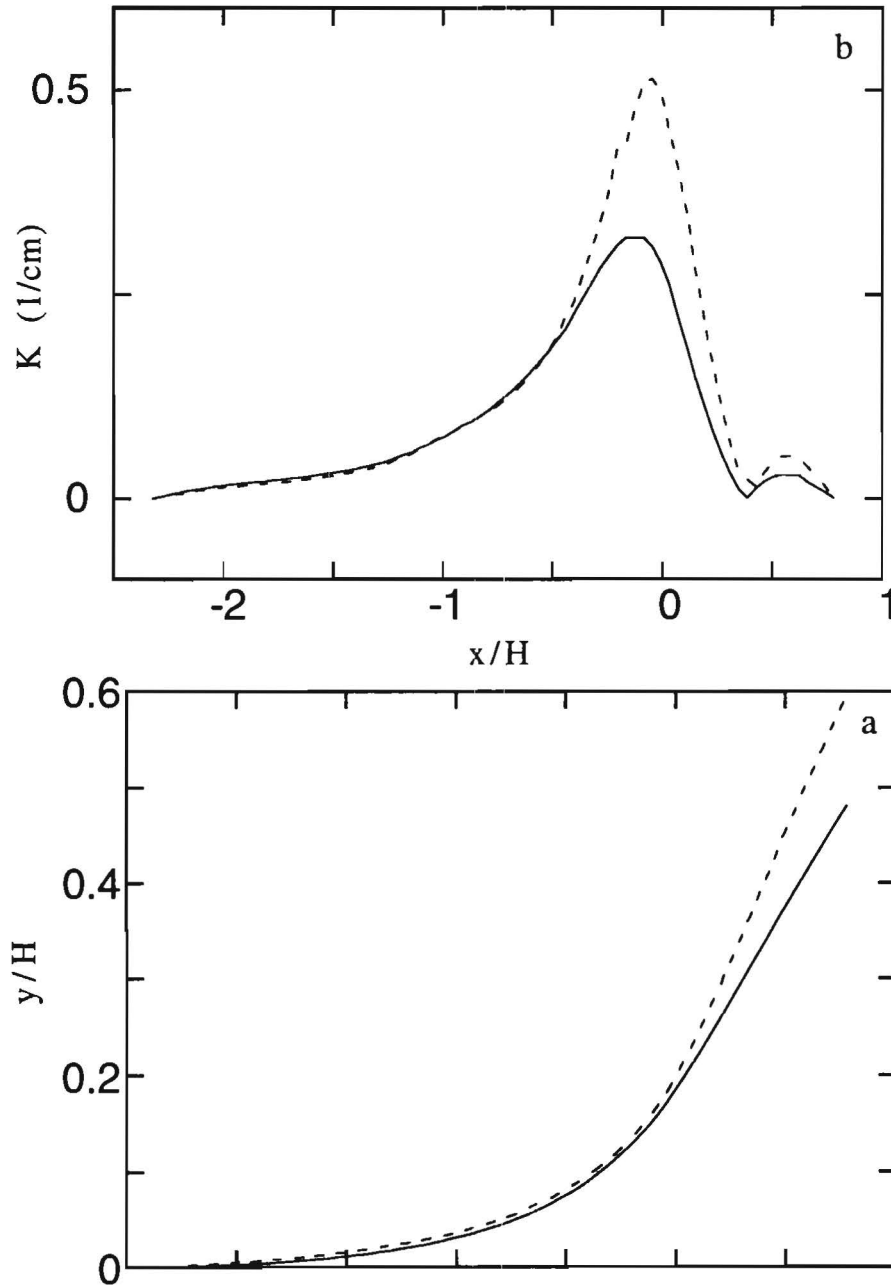


Figure 5



Assuming, as mentioned above, that the vectoring of the primary jet results from the formation of a low pressure region and of a recirculating flow bubble between the two jets and near the exit plane, it may be argued that the vectoring is a result of a balance between the pressure force and the momentum of the primary jet. The static pressure near the downstream edge of the primary jet conduit on the actuator side was measured for various values of  $P$  and for different speeds of the primary jet. This pressure is normally below atmospheric when both jets are operational and decreases with increasing momentum flux of the synthetic jet. Furthermore, the pressure also decreases almost linearly with increasing Reynolds number of the primary jet. When all the data are plotted in dimensionless form, it is found that  $\alpha \propto \text{Re}_H P^{-4/3}$ . (Figure 6).

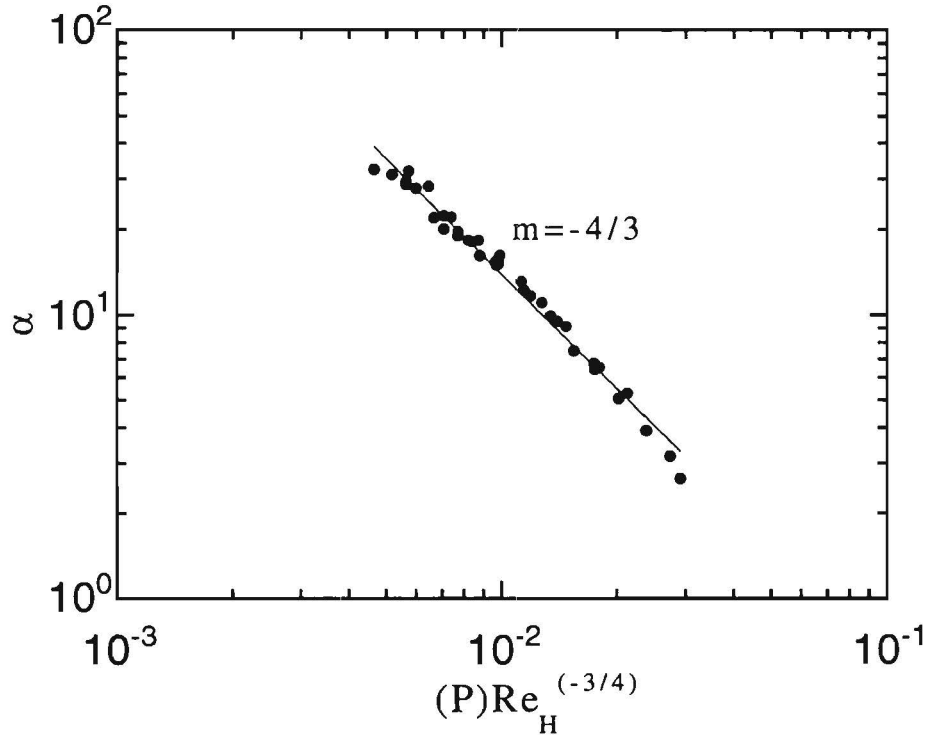


Figure 6

### III. Conclusions

The present measurements have demonstrated that the vectoring angle does not depend uniquely on the momentum ratio between the primary and synthetic jets and that for a given momentum ratio, the vectoring angle increases with the momentum of the primary jet. This means that for a given momentum ratio, the vectoring angle increases with

decreasing pressure within the low pressure recirculating flow region between the two jets and that the vectoring is a result of a balance between the pressure force and the momentum of the primary jet. For a given primary jet Reynolds number, the pressure between the two jets decreases further with increasing momentum flux of the synthetic jet, and, for a given synthetic jet momentum, the pressure decreases with increasing primary jet Reynolds number.